J. Membrane Biol. 13, 299–322 (1973)

Current-Induced Voltage Transients in *Necturus* Proximal Tubule

Kenneth R. Spring

Department of Physiology, Yale University School of Medicine, 333 Cedar Street, New Haven, Connecticut 06510

Received 12 March 1973

Summary. Transients in the potential difference spontaneously developed by the *Necturus* proximal tubule were characterized during and after voltage or current clamp commands. These voltage transients were adequately fitted by an exponential function similar to that describing the ionic charging of a leaky fluid capacitance and were slower during clamp periods ($t\frac{1}{2}=0.98$ min) than after release of the clamp ($t\frac{1}{2}=0.46$ min). Changes in luminal ionic composition and cellular membrane potential were ruled out as sources of generation of the voltage transients. The volume of the fluid compartment in which concentration changes occurred was calculated from the electrical data and it was concluded that the extracellular shunt path was the principal site of the concentration changes which resulted in voltage transients. A fall in transepithelial resistance to nearly one-half its original value occurred during hyperpolarizing commands while depolarizing commands did not significantly alter resistance. The resistance changes were interpreted as indicative of the degree of widening of the lateral intercellular spaces caused by fluid accumulation or depletion. The important role of the lateral space dimensions in determining epithelial permeability, electrical resistance and voltage transients was pointed out, and a new electrical analogue model of the shunt path was proposed.

The passage of electric current through the *Necturus* proximal tubular epithelium by the method of voltage clamping leads to volume flows and alterations in the transepithelial potential difference spontaneously produced by the epithelium. Transients in spontaneous potential difference (PD) were observed following the release of voltage clamp commands and appeared as a return of the spontaneous PD to its original value after having been displaced in the direction of the command potential. Apparent increases in proximal tubular electrical resistance and hysteresis of low frequency current-voltage diagrams were also noted and suggested changes in both transepithelial resistance and electromotive force during the course of voltage clamp experiments [23]. The voltage transients were similar in appearance to the "polarization PD's" observed by Wedner and Diamond [24] in rabbit

gallbladder after the cessation of a constant current command, which were assumed to be related to alterations in intraepithelial ion concentration induced by current passage. Barry and Hope [2, 3] described alterations in ionic concentration differences across the cell wall of the alga, *Chara*, which were induced by the passage of electric current. These concentration differences resulted in changes in transcellular PD and water flow. A similar explanation is offered here for the alterations in spontaneous PD and volume flow observed during and after current passage in *Necturus* proximal tubule.

I studied the voltage and resistance changes which accompany the passage of electric current through the epithelium of the *Necturus* proximal tubule under conditions of voltage and current clamp. In addition, I analyzed the volume flows associated with these transients and with the application of constant current or voltage commands. These phenomena were characterized to delineate the dynamic behavior of the epithelium and to further elucidate the mechanism of fluid transport in the proximal tubule. The results which follow indicate that current passage causes alterations in the salt concentrations of the lateral intercellular spaces and that these concentration changes in turn lead to PD transients and volume flows. The information obtained from the analysis of the time course, direction and magnitude of the voltage and resistance transients is used in the second paper of this pair [22] to estimate some of the transport parameters of the epithelium. The conductance and permeability increases which accompany hyperpolarization of the transepithelial PD (increasing luminal negativity) are explained in this and the succeeding paper as the consequences of increasing the width of the lateral intercellular spaces.

Materials and Methods

Adult *Necturus* maculosus of both sexes were obtained from Mogul Ed. Corp., Oshkosh, Wisconsin and stored at 17 to 21 °C in a large tank. They were anesthetized by immersion in a 0.1% tricaine methane sulfonate solution (Ayerst Lab, New York) at neutral pH and room temperature (ca. 23 °C) until skin reflexes disappeared. After removal from the anesthetic they were prepared for micropuncture as previously described [23]. All experiments were performed with the animal's body temperature at 20 ± 1 °C. The method for micropuncture and clamping was essentially similar to that described previously and will be only briefly outlined here. Large droplets of *Necturus* Ringer's solution were injected into long, straight, oil-filled segments of late proximal tubule, in vivo, and inserted into those droplets were both an axial current electrode and a 3 M KCL-filled glass microelectrode for recording transepithelial PD. The platinized tungsten axial wire electrode was advanced into the droplet through the barrel of a sharpened micropipette and was connected to the output of a voltage/current clamp. The indifferent electrode for the current circuit, a large, platinum black, silver chloride wire lying under the kidney was held at virtual ground by the current amplifier and

served as the current-measuring electrode. Constant current or voltage commands were applied to the epithelium through the axial wire while fluid reabsorption was measured simultaneously by direct microscopic observation of the change in length of the droplet of Ringer's solution contained between the oil columns.

The axial electrode was similar in mechanical design to that described by Spring [21] except that its diameter was reduced by electropolishing in 0.1 N KOH (4 V D-C for 2 min, with a carbon rod as the cathode) and its surface, after cleaning in acid, was electroplated with gold (Sel-Rex solution, Autronex, Nutley, N. J., 4-V monophasic pulses, 10 msec duration, 38/sec for 30 sec, platinum wire as the anode) before platinization. The final electrode was about 8 μm in diameter and the platinum black layer did not scrape off under any experimental circumstances. The small diameter of the axial wire, combined with the utilization of thin wall glass tubing (#33 borosolicate, o. d. 1 mm, wall thickness 0.15 mm Friedrich-Dimmock, Millville, N. J.) to fabricate the micropipettes enabled a reduction in the outside diameter of the pipettes to 20 to 25 μm.

The equipment used for measurement of PD's and the voltage/current clamp also differed from those used previously. PD's were measured with 3 M KCl-filled glass microelectrodes mounted in a silver chloride half-cell; a Ringer's-soaked wick inserted into another half-cell served as the reference electrode, which was positioned as close as possible to the tubule under study. The half-cells were connected to a dual electrometer with capacitance compensation, variable D-C offset, and impedance monitoring capabilities for each amplifier (W 750, WP Instruments, Hamden, Connecticut). The rise-time of either channel with a 20 MΩ glass microelectrode in each was less than 7 μsec. The sum of the outputs of each channel, or the individual output in some cases, was used as the input signal to the control amplifier of the clamp circuit. The voltage/current clamp had sufficient speed and stability for the entire circuit to display a rise-time of 20 μsec and an overall gain of 10,000. The current and voltage outputs of the clamp amplifiers were displayed on an oscilloscope (Tektronix 502 A, Beaverton, Oregon), recorded on a chart recorder (Gulton-Technirite, East Greenwich, Rhode Island) or on an oscilloscope camera (model C4N Kymograph camera, Grass Instruments, Quincy, Massachusetts). The voltage channel was also monitored with an audio monitor during electrode insertion and measurement of volume flows.

Split droplets were formed with a glucose-free, bicarbonate Ringer's solution similar to that used previously [23]. Determination of droplet length was made continuously at 128 × (Leitz Wetzlar, Rockleigh, N. J.) with the aid of an ocular micrometer disc or filar eyepiece (Leitz). Optically determined droplet length was depicted on the chart recorder as the ratio of the length measured from the ends of each oil column at any time $L(t)$ to its length at initial observation $L(0)$.

The experimental procedure for localization of the microelectrode and recording transients differed somewhat from that of voltage clamp experiments. After selection of a suitable tubule for micropuncture, a long proximal oil block was inserted (mineral oil 330 cp, droplet length at least 10 tubule diameters), and the tubular pipette containing its axial wire inserted into the most proximal portion of the segment to be studied. The oil column was adjusted until it barely covered the sharpened end of the tubular pipette and the axial wire was advanced slightly beyond the oil meniscus (Fig. 1 *A*). Constant current pulses of small amplitude (100 nAmp, 1 msec duration, 20/sec) were passed from the axial wire down the length of the cable-like tubule. A voltage-measuring electrode, placed on the renal surface, detects these pulses as voltage deflections proportional to the intervening tissue and solution resistances. Each current pulse was followed after a brief delay by an impedance test pulse from a second voltage source to the microelectrode input of the electrometer. Two pulses appeared on the oscilloscope screen as shown in Fig. 1: the first, the "coupling" pulse from axial wire to microelectrode; the second, the impedance test of the microelectrode itself. This sequence served two purposes:

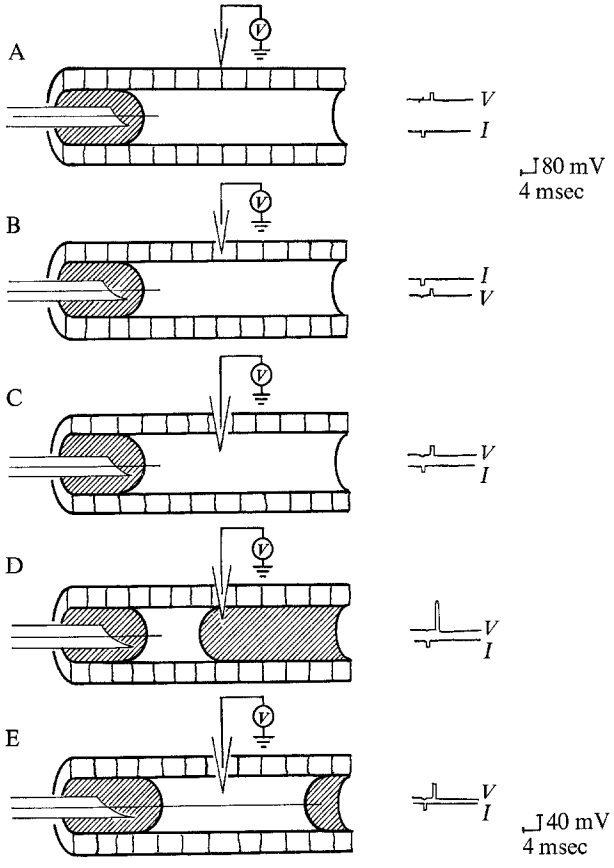

Fig. 1. Method for electrode localization and impedance monitoring in a proximal tubule prior to the passage of oil through the region under study. In *A* the voltage-measuring microelectrode rests on the kidney surface and shows minimal coupling (upper trace) with the constant current pulse from the axial wire (lower trace). The second pulse gives a measure of the electrode impedance (1 mV = 1 MΩ). In *B* microelectrode has entered a tubule cell with a resting membrane PD of −85 mV. In *C* the electrode is in the tubule lumen; in *D* oil covers the microelectrode tip, reducing coupling and increasing impedance. In *E* the split droplet has been moved to the region of the microelectrode and the axial wire advanced across the drop

coupling can be used as a method of localization of the microelectrode in the lumen [12] and impedance measurements give a constant record of the state of the electrode tip [23]. Luminal localization of the microelectrode was verified in several ways: 1) coupling is maximal; 2) impedance returns to original values recorded on the renal surface; 3) advancement of the oil column with subsequent "splitting" by the injection of Ringer's solution from the tubular pipette causes the sequence of changes shown in Fig. 1 *D* and *E*. This approach also gives us the opportunity to measure transepithelial PD in a segment prior to and after the passage of an oil column through it.

After the droplet was injected, the axial wire was advanced across the droplet and control records were made of PD and volume flux (J_v). Triangular wave constant current

commands were passed through the axial wire at a frequency of 5/sec and varying amplitude (100 to 400 nAmp) periodically to measure the transepithelial resistance. These small perturbations in current result in a linear displacement of the transepithelial PD and were used along with measurements of the tubular dimensions to calculate the "instantaneous" resistance, R_{ins}, during the course of an experiment.

The data immediately available from a voltage or current clamp experiment were then: 1) spontaneous transepithelial PD, E_{spon}; 2) overall or command transepithelial PD, E_{tot}; 3) electric current, I; 4) instantaneous resistance, R_{ins}; 5) volume flux, J_v. These data were analyzed by use of a digital computer (model 7094/7040, IBM, New York) as follows: E_{spon} and E_{tot} were fitted, after a suitable transformation described in the results section of this paper, by the method of least-squares; current per unit area, I/A, was calculated from the observed current and the area determined from the droplet dimensions; J_v was determined by the method of least-squares from the transformation of droplet dimensions suggested by Nakajima *et al.* [17]; R_{ins} was divided by the area, A, calculated from the least-squares line for J_v and the droplet dimensions, and expressed as specific resistance for comparison with the "steady state" or chord resistance, R_{ss}, which was calculated from the expression:

$$R_{ss}=[E_{tot}-E_{spon}]/I/A \tag{1}$$

where E_{tot}, E_{spon} and A are calculated from the coefficients of their respective least-squares lines. Current density was integrated by a numerical method [quadrature, 14] to determine the total charge transferred at any time during a voltage or current clamp. This approach was particularly useful in calculations involving voltage clamps since current density changes considerably in the first minute of clamping.

During saline-loading experiments, extracellular fluid volume was expanded by the infusion of Ringer's solution into the ventral abdominal vein at a rate of 4 ml/hr for no more than 2 hr. All determinations were made after a 1-hr period of equilibration to the saline infusion.

Data are presented as mean value and standard error; statistical analysis and subsequent mathematical modeling calculations were carried out on an IBM 370/155 digital computer.

Results

Temperature Effects

Since the animals in this study were stored and micropunctured at a higher ambient temperature (20 °C) than in the previous voltage clamp experiments (15 °C), the values of peritubular (intracellular) PD and transepithelial PD were re-evaluated. The results in Table 1 (top) show that peritubular PD increased significantly over this temperature range, while transepithelial PD remained unchanged. As a check on the validity of these results, an experiment was carried out in which one animal's body temperature was reduced from 20 to 15 °C and peritubular membrane potentials compared. As seen in the lower portion of Table 1, a reduction of only 5 °C again caused a significant decline in peritubular membrane PD. The magnitude of the PD changes which accompany such small alterations in temperature are not consistent with the effects expected from the coefficients of the Nernst equation.

Table 1. Temperature dependence of PD's in proximal tubule

PD	20 °C	15 °C	*t* test
Peritubular PD	-72.6 ± 0.95 (100)[a]	-62.7 ± 0.82 (198)	$p < 0.0005$
Transepithelial PD	-10.3 ± 0.85 (20)	-12.6 ± 0.90 (52)	ns
Peritubular PD (Cooling same animal)	-78.2 ± 1.56 (5)	-66.1 ± 2.55 (8)	$p < 0.0005$

[a] Number of observations in parentheses.

Voltage Transients

Study of the voltage transients during and after current passage is divided into three areas: 1) characterization of the time course of PD transients under voltage and current clamp; 2) description of the resistance changes which accompany the PD transients and alter their magnitude and time course; 3) localization of the site of generation of the transients.

Time Course of Voltage Transients

Examples of transients during voltage and current clamps are shown in Fig. 2. The time course of voltage change appeared to be an exponential approach to an asymptote. The voltage transients were determined by inspection to conform generally to the following equation:

$$V(t) = V(\infty) - (V(\infty) - V(0))\, e^{-kt} \tag{2}$$

where $V(t)$ is the value of the transepithelial PD at any time, $V(\infty)$ is the asymptotic value, $V(0)$ the value at time zero, and k the rate constant of voltage change. When $\ln (V(\infty) - V(t))$ is plotted against time, the slope of the line gives k and the intercept equals $(V(\infty) - V(0))$. The optimum value of $V(\infty)$ results in a minimum sum of squares of deviations of experimental points from the calculated values. The application of Eq. (2) to the experimental transients assumes that the rate constant does not change during the course of the transient. The results of this transformation must be regarded as an approximation of the experimental curve in which the rate constant also undergoes time dependent alterations in some cases (*see below*), and the resultant voltage changes cannot be readily linearized. The results of fitting the transients by Eq. (2) for both voltage and current clamps are shown in Table 2. The pooled PD transients when the clamp was "on" were significantly slower than the relaxation transients observed when the clamp

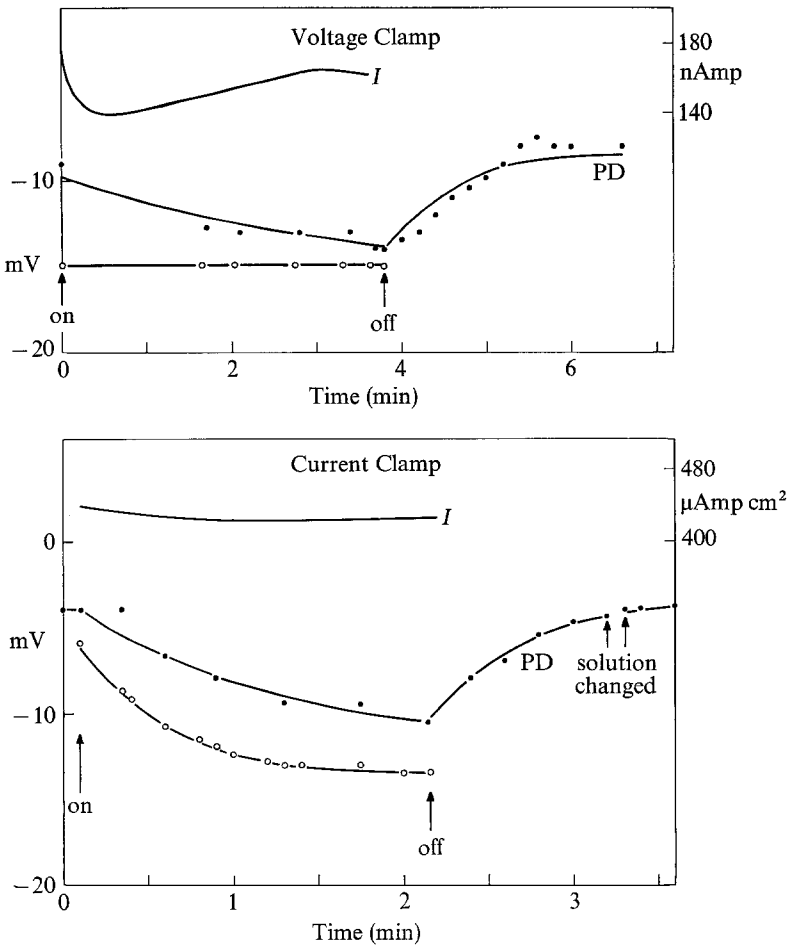

Fig. 2. Current and voltage changes during voltage clamp (top) and current clamp (bottom) commands. The filled circles (•) indicate experimentally determined spontaneous PD, the open circles (◦) experimentally measured overall PD. Lines through the PD points are drawn by the method of least-squares. In the upper record I is total current since the drop dimensions were not recorded; in the lower record I is expressed as current density with continuous correction for alteration in droplet size. At 3.2 min in the lower record a new split drop was forced through the tubule lumen to observe the effects of stirring and solution change

was turned "off" (Table 2). This was confirmed by a paired t test of spontaneous PD transients during and after individual current clamp commands ($n = 20$, $p < 0.02$ for k and $t\frac{1}{2}$), and with voltage clamp commands ($n = 16$, $p < 0.05$ for $t\frac{1}{2}$, n. s. for k). There was a trend for depolarizing (lumen less negative) commands to cause a more rapid alteration of spontaneous PD than hyperpolarizing (lumen more negative) inputs, but this difference was not signi-

Table 2. Spontaneous PD transients pooled from voltage and current clamps

Command	n	k (min^{-1})	$t\frac{1}{2}$ (min)	t test	Correlation coefficient
"Off"	57	-1.84 ± 0.19	0.46 ± 0.04		0.87 ± 0.02
Depolarizing	16	-1.68 ± 0.30	0.66 ± 0.11	$p<0.05$	0.83 ± 0.03
Hyperpolarizing	29	-1.20 ± 0.29	1.16 ± 0.19	$p<0.001$	0.86 ± 0.02
"On" pooled	45	-1.37 ± 0.22	0.98 ± 0.13	$p<0.001$	

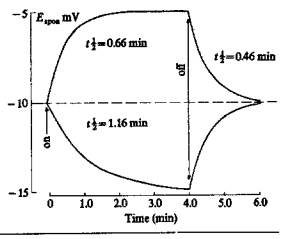

Shown in the inset are average transients computed from the pooled time constants in the table for a voltage deflection of 5 mV from the normally pertaining spontaneous PD.

Table 3. Overall PD transients during current clamp

Command	n	k (min^{-1})	t test	$t\frac{1}{2}$ (min)	t test
Depolarizing	7	-2.65 ± 0.64	$p<0.01$	0.35 ± 0.06	$p<0.01$
Hyperpolarizing	16	-1.12 ± 0.17		0.76 ± 0.07	
Pooled	23	-1.58 ± 0.27		0.64 ± 0.07	

ficant. Current clamp transients were virtually identical to those during voltage clamp and, after statistics did not reveal any significant differences between the two groups, were pooled for presentation in Table 2. Although the spontaneous PD transients did not differ in time course from a voltage to current clamp, the total PD's were fundamentally different. During a voltage clamp the total PD is the variable controlled and clamping current displays a transient which is the inverse of the spontaneous PD transient (Fig. 2, top). Since the current clamp involves the passage of a constant current, total PD is allowed to vary and also displays a transient (Fig. 2, bottom). The transient in total PD under current clamp was somewhat faster than the spontaneous PD results and exhibited a significant difference between depolarizing and hyperpolarizing commands (Table 3).

In summary, the voltage transient analysis demonstrated that: 1) transients during voltage and current clamp were essentially similar; 2) "on" transients were significantly slower than "off" transients; and 3) hyperpolarizing and depolarizing commands gave transients which tended to different time courses, but not significantly.

Experiments were also performed to determine the effects of isotonic volume expansion on the time course of the transients during current clamp. The result of these experiments was that the rate constants observed during volume expansion did not differ significantly from control values. (E_{spon} "on" $t\frac{1}{2} = 0.98 \pm 0.18$ min, E_{spon} "off" $t\frac{1}{2} = 0.39 \pm 0.4$ min, n = 16).

Resistance Determination

As mentioned in Materials and Methods, transepithelial resistance could be determined in two different ways. The instantaneous resistance, R_{ins}, calculated from small perturbations was used as a check on the value of the steady-state resistance, R_{ss}. The resistance determined at time zero by both methods did not differ significantly: control tubules $40.9 \pm 6.7\ \Omega\ cm^2$ (n = 39); volume expansion $30.8 \pm 4.5\ \Omega\ cm^2$ (n = 18). Calculated transepithelial resistance often displayed transients similar in appearance to the voltage transients. During hyperpolarizing commands, in particular, a striking parallelism between voltage and resistance changes could be observed (Fig. 3, top). The similarity of the time dependence of voltage and resistance changes during hyperpolarizing commands was further substantiated by fitting the resistance change with the same exponential function that described the voltage transients. The results of this approach are shown in Table 4, where it may be seen that the $t\frac{1}{2}$ of resistance change was significantly smaller than that of the voltage transient. Such parallel time courses were rarely observed during depolarizing commands, where more commonly resistance did not change significantly while voltage transients occurred (Fig. 3, bottom). The general pattern which emerged is a fall in resistance during hyperpolarizing commands ($R(0)/R(\infty) = 1.8$, significantly greater than 1, $p < 0.05$) and no significant change during depolarizing commands ($R(0)/R(\infty) = 1.24$, not significantly different from 1). A steady-state current-voltage diagram of the epithelium would be nonlinear because of the fall in resistance during hyperpolarizing commands.

Resistance determined by the perturbation method exhibited transients that support the validity of the changes in the steady-state values (Fig. 4). Regardless of the time-dependent alterations in steady-state resistance which took place, the instantaneous current-voltage plot of the epithelium

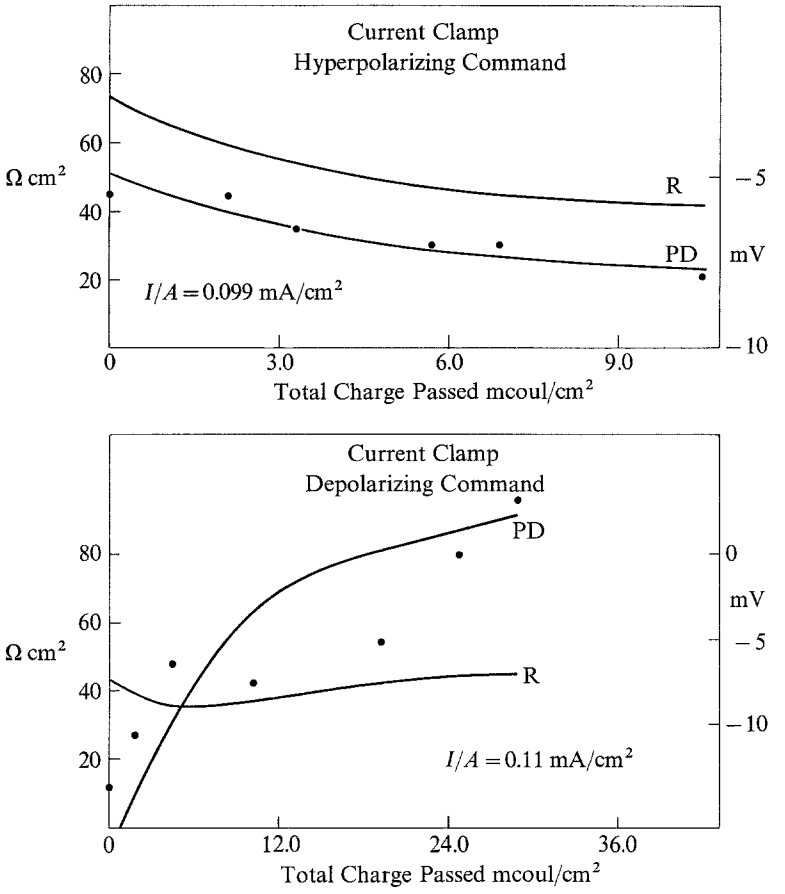

Fig. 3. Transepithelial resistance changes during hyperpolarizing (top) and depolarizing (bottom) commands. Spontaneous PD transients are shown for each case with lines fitted by the method of least-squares. The abscissa is the integral of the applied current density expressed as charge transferred per cm^2 of epithelium

Table 4. Comparison of resistance and spontaneous PD transients during hyperpolarizing command

	n	k (min^{-1})	t test	$t\frac{1}{2}$ (min)	t test	Correlation coefficient
Resistance	27	-1.59 ± 0.18		0.58 ± 0.06		0.84 ± 0.03
Voltage	29	-1.20 ± 0.29	ns	1.16 ± 0.19	$p < 0.01$	0.86 ± 0.02

was always linear during a transient. All resistance changes were reversible and transients of resistance during off commands were observed. It should be noted here that this observed decrease in steady-state resistance is not

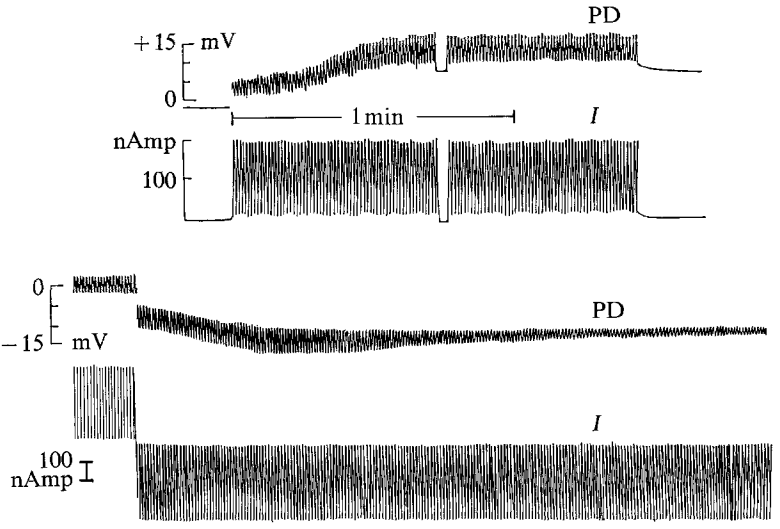

Fig. 4. Changes in transepithelial resistance determined by triangular wave perturbations during depolarizing current clamp (top) and hyperpolarizing current clamp (bottom)

contradictory to the previous observation [23] that "apparent" transepithelial resistance, R_{ss}, increased during voltage clamp experiments. In the previous experiments spontaneous PD was not monitored during a voltage clamp period. The clamp current decreases with time as E_{spon} moves toward E_{tot} since the ΔV required is smaller than at time zero (*see* Fig. 2, top). Steady-state resistance, calculating from $\Delta V/I/A$ and assuming a constant value of ΔV, appears to increase as previously described. Without measurements of the alterations in spontaneous PD which accompany the passage of current a similar conclusion might have been reached from the present data.

Localization of the Site of PD Transients

As part of an attempt to more precisely localize the site of the voltage transient observed during clamping, two series of experiments were done. In one, peritubular membrane PD was monitored during a voltage transient; in the second, a new split droplet was introduced into the tubule during the relaxation voltage transient after the clamp had been turned off.

In a few experiments simultaneous records of transepithelial and peritubular membrane PD were made during current clamp (Fig. 5). In most cases, however, a known current density was passed through the epithelium, without determination of the transepithelial PD, while monitoring the peri-

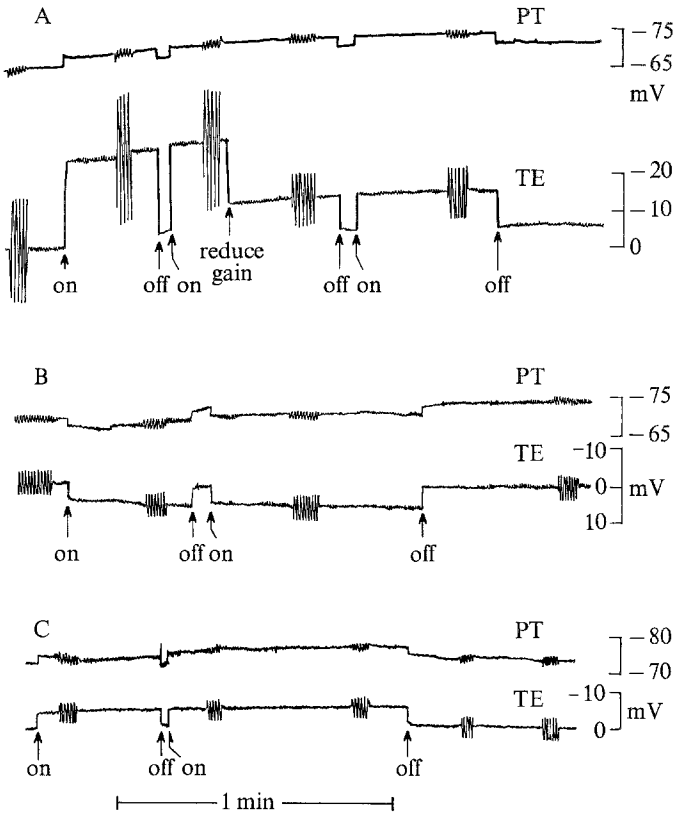

Fig. 5. Records of simultaneous measurements of transepithelial (TE) and peritubular (PT) membrane PD's in the same region of tubule. In *A* a hyperpolarizing command (210 nAmp) is applied through the axial wire. Triangular wave perturbations (320 nAmp) for the measurement of resistance are included as well as periodic release of the clamp at points indicated by the arrows. In *B* a depolarizing command of 200 nAmp was applied, and in *C* a hyperpolarizing command of 200 nAmp. Voltage gain, with the exception of the first portion of the TE trace in *A*, is the same for both PT and TE measurements

tubular PD of cells lining the droplet. The primary goal was to observe any transients in peritubular PD which correspond to those in the transepithelial PD and not to determine the properties of the peritubular membrane. In Table 5 I report the direction of the voltage changes observed and conclude that there does not seem to be a consistent transient in peritubular PD during a transepithelial voltage transient.

The injection of a new droplet into the lumen from the tubular pipette during a transient simulates the experiment of Wedner and Diamond [24] in which solutions bathing the rabbit gallbladder were replaced during a

Table 5. Changes in peritubular membrane PD during current clamp

Command	No. of obs.	+	−	nc
Hyperpolarizing	19	5	7	7
Depolarizing	18	10	1	7

Direction of peritubular membrane voltage change compared to the direction of the transepithelial voltage transient caused by current passage. (+) indicates a peritubular transient in the same direction as transepithelial, (−) indicates a transient in the opposite direction, and (nc) indicates no discernable transient in peritubular PD.

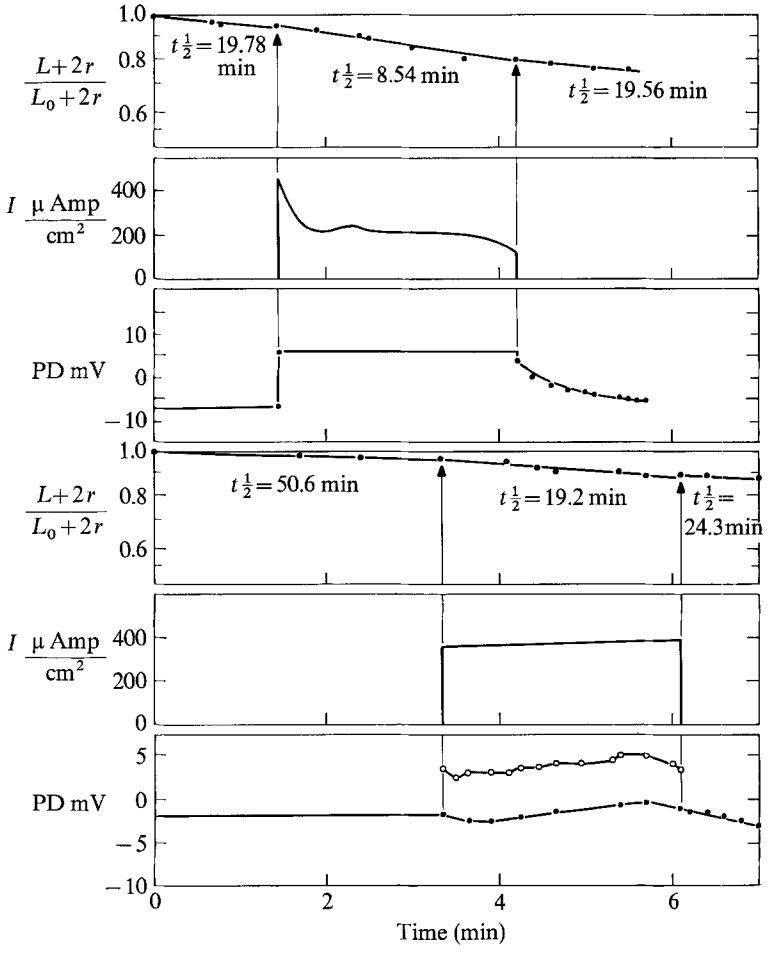

Fig. 6. Experimental records of droplet shrinkage (top trace), electric current density (center trace) and PD (lower trace) during both voltage (top half) and current clamp (bottom half). The half times for fluid reabsorption during each period are indicated below the respective sections of the drop shrinkage curve

PD transient. As shown in Fig. 2, the injection of a second split droplet does not alter the time course or amplitude of the PD transient. In nine other experiments injection of a second droplet at various times after both voltage and current clamps support the conclusion that the PD transient is not caused by luminal unstirred layers or abnormal ionic composition of the luminal solution.

Volume Flows

During the passage of electric current, fluid flow caused by that current was toward the cathode at a rate roughly proportional to the current density. Under voltage clamp, J_v usually became constant in the first few seconds and continued unchanged until the command was altered (Fig. 6, and ref. [23]). Under constant current clamp, J_v was similar but smaller in magnitude and often did not assume a uniform rate for a minute or more. The more rapid establishment of nearly constant J_v under voltage clamp than under current clamp was probably a consequence of the high initial current density in the first minute of voltage clamping (Fig. 6).

The pattern of fluid flux as a function of applied PD during voltage clamp was similar to that previously reported [23]. For a similar voltage deflection, with the luminal electrode as the cathode (hyperpolarization), J_v was greater than when the lumen was the anode (depolarization). Current clamp results were less easily depicted since J_v was a function of the applied current density and the relative resistance of the epithelium. The theoretical basis for determination of volume flow during the application of a constant current or voltage is considered, in detail, in the subsequent paper [22].

Discussion

The features of the voltage transients may be summarized as follows: 1) current passage induces spontaneous PD transients in the same direction as the overall voltage; 2) these PD transients build and decay in an exponential fashion; 3) changes in luminal solution do not affect their time course or amplitude; 4) peritubular membrane potential changes little if at all during such a transient; 5) relaxation of current-induced voltage transients is faster than their buildup; 6) there may be simultaneous transients in transepithelial resistance. These observations suggest that the voltage transients are a consequence of intraepithelial concentration changes caused by electric current passage. The exponential behavior of the transients is

similar to the charging and discharging of compartment in the epithelium in the way a leaky electrical capacitance is charged or discharged through a resistance. The failure of changes in luminal solution to affect the transients rules out the luminal compartment as the site of these concentration changes. The negligible alterations in peritubular membrane PD during current passage show that little current flows through that barrier and that significant changes in intracellular composition are not caused by the passage of current.

The electrical analogue model of the proximal tubule first presented by Boulpaep [6] and a similar and more detailed model of the intestinal epithelium by Rose and Schultz [20] both predict that the majority of an applied electric current flows through the shunt pathway and that transepithelial electrical resistance is principally determined by the shunt resistance. Subsequent investigation by Frömter and Diamond [13] of the current spread in *Necturus* gallbladder confirmed the high current density in the extracellular shunt path. The effect of applied current on the ionic composition of the lateral intercellular spaces was considered by Wedner and Diamond [24] in rabbit gallbladder and the basal-lateral spaces were proposed as the site of generation of the "polarization PD's" observed during and after current passage. The calculations of Rose and Schultz [20] based on their electrical analogue model, state in a simplified form, that the transepithelial PD is given by:

$$V=\left[\mathrm{EMF}_{\mathrm{cell}}\frac{R_{\mathrm{shunt}}}{R_{\mathrm{tot}}}\right]+\left[\mathrm{EMF}_{\mathrm{shunt}}\frac{R_{\mathrm{cell}}}{R_{\mathrm{tot}}}\right] \tag{3}$$

where $\mathrm{EMF}_{\mathrm{cell}}$ is the total electromotive force of the luminal and peritubular potential generators, $\mathrm{EMF}_{\mathrm{shunt}}$ is the electromotive force developed by the concentration gradients across the shunt path, R_{shunt} is the resistance of the shunt path, R_{cell} the sum of the peritubular and luminal membrane resistances in series, and $R_{\mathrm{tot}}=R_{\mathrm{cell}}+R_{\mathrm{shunt}}$. From the data of Boulpaep [7] and Windhager, Boulpaep and Giebisch [26] the resistances have the following values: $R_{\mathrm{shunt}}=70\ \Omega\ \mathrm{cm}^2$, $R_{\mathrm{cell}}=7900\ \Omega\ \mathrm{cm}^2$, $R_{\mathrm{tot}}=7970\ \Omega\ \mathrm{cm}^2$. Then V is given by:

$$V=0.009\ \mathrm{EMF}_{\mathrm{cell}}+0.991\ \mathrm{EMF}_{\mathrm{shunt}}.$$

A change in $\mathrm{EMF}_{\mathrm{shunt}}$ is much more effective in altering V than are shifts in $\mathrm{EMF}_{\mathrm{cell}}$. This does not imply that the spontaneous transepithelial PD is normally generated by $\mathrm{EMF}_{\mathrm{shunt}}$ but rather that changes in V are more

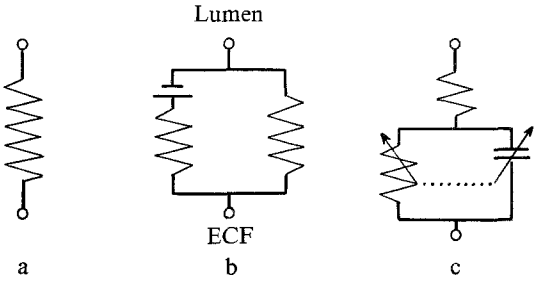

Fig. 7. Electrical equivalent circuits of the shunt pathway in epithelia. (*a*) shunt in *Necturus* proximal tubule [6], (*b*) small intestine shunt analogue [20], (*c*) proposed *Necturus* shunt path model

readily achieved by alterations in that electromotive force. In the intestine [11, 20] and in the proximal tubule [22] EMF_{shunt} actually is in the opposite direction to the normally observed V and opposes the PD spontaneously developed by EMF_{cell}. The analogue also indicates that the peritubular membrane PD would be influenced only to a small extent by alterations in EMF_{shunt} alone.[1] Previous investigations indicate that the peritubular membrane resistance is considerably smaller than the luminal [7, 26], a conclusion which is substantiated by Fig. 6 from which it may be calculated that the resistance of the luminal membrane is two to three times greater than that of the peritubular. I conclude that the applied current goes primarily through the shunt path and that the transients in transepithelial PD are most probably produced by changes in the EMF generated by salt gradients along the shunt pathway rather than by changes in cellular EMF's. Careful consideration must then be given to the electrical equivalent circuit for the shunt path because of its major role in current related phenomena.

Boulpaep [6] depicted the shunt pathway as a fixed resistance as shown in Fig. 7*a*. Rose and Schultz [20] suggested a more complex circuit consisting of a fixed resistance in parallel with an EMF and its series resistance (Fig. 7*b*). On the basis of the present results and those discussed below, I chose to represent the shunt by the circuit in Fig. 7*c*. This analogue consists of three electrical elements: parallel, variable resistance and capacitance, in series with a fixed (or less variable) resistance. Representation of the shunt by several electrical elements does not mean that the physical system is as complex as the analogue. Actually the parallel elements, resistance and

1 Δ peritubular PD is proportional to $\Delta EMF_{shunt}\left(\frac{R_{peritubular}}{R_{tot}}\right)$, where $R_{peritubular}$ is estimated as $\approx 3500\ \Omega\ cm^2$ and $R_{tot} \approx 8000\ \Omega\ cm^2$ [7, 26].

capacitance, may be the properties of one epithelial component, the lateral intercellular spaces. It may be seen in Figs. 2–4 that the EMF and resistance of the shunt path are variable, and as shown below, the capacitance may also be altered. In this model, the PD generated in the shunt path is not due to an EMF as suggested by Rose and Schultz ([20], and Fig. 7*b*) but to the amount of ionic charge (cations + anions) on the shunt capacitor. This capacitor may be charged by the passage of electric current or by active transport of salt out of the adjacent tubule cells. The values of the electrical elements in Fig. 7*c* may change depending on the magnitude and direction of the applied electric current; the nature of these variations and their interrelationships constitute the principal objects of this investigation.

A general understanding of the meaning of changes in the observed voltage transients may be obtained from the circuit of Fig. 7*c*, in which it is assumed that the EMF of the shunt path is only due to the amount of ionic charge on the shunt capacitance, C. If the two resistances are lumped together as a single value, R, the rate constant of the voltage transients, k in Eq. (2), is then equal to $1/RC$. Variations in k must be due to alterations in either R or C. The applicable experimental data for overall voltage transients (Tables 2 and 3) yield RC products of 22.6 sec for depolarizing commands, 53.5 sec for hyperpolarizing commands, and 32.6 sec for "off" commands. During depolarizing commands R does not change or decreases slightly from control (Figs. 3 and 4) and the decrease in the time constant may also be due to a fall in C. Since hyperpolarizing commands prolong the time constant and decrease resistance, capacitance must then increase to a greater extent. When the clamp is "off" the charged shunt capacitor discharges through its parallel resistance and gives a time constant which depends on the value of that resistance as well as the value of C. A likely physical analogue of the above variations in R and C is a widening of the lateral intercellular spaces during hyperpolarizing commands which results in an increased shunt volume (capacitance) and a decreased resistance. During depolarizing or "off" commands the lateral spaces collapse resulting in a decreased volume and increased (or unchanged) resistance. In these cases I have assumed little or no change in the series resistance during current clamps. The fixed series resistance in Fig. 7*c*, whose physical analogue is the tight junction, is required in the model since C increases more than R during widening of the lateral spaces. It should be noted that changes only in the series resistance could also account for much of the resistive variation observed experimentally; however, I have assumed fixed dimensions and properties of the tight junctions in the discussion which follows. It is apparent from the long time constants of the voltage transients that

the equivalent of immense electrical capacitances exist within the epithelium. Such large capacitances must be properties of the ionic charge and discharge of fluid compartments rather than dielectric capacitors merely on the basis of the available membrane surface area. An essentially similar interpretation of the long time constant voltage transients of gastric mucosa was offered by Noyes and Rehm [18].

If the shunt path is analogous to an electrical capacitor in its ability to store and give up ionic charge, there should be a linear relationship between the amount of charge passed (ΔQ) and the magnitude of the resultant voltage transient (ΔV). For an ideal capacitor, the equation is

$$\Delta V = \Delta Q / C \tag{4}$$

where C is the equivalent electrical capacitance of the fluid compartment. Since the shunt is a "leaky" capacitor, most of the charge passed is lost through resistive paths. The ΔQ of interest is only that portion of the total charge passed which goes to charge the capacitance. This value is calculated by subtracting the resistive current from the total and integrating the remainder using a numerical computer method. Since the resistance of the epithelium changes during current passage in some cases, the larger resistive current was recalculated at short intervals to avoid errors in estimating the smaller capacitative current. Fig. 8 shows the relationship between ΔQ and ΔV at the end of each clamp period for control and volume-expanded animals. The equivalent electrical capacitance for the control animals was 5.4×10^{-3} F/cm^2 and in volume expansion this rose to 7.4×10^{-3} F/cm^2 (the difference in slopes of these two least-square lines is of borderline significance, $0.05 < p < 0.1$). The electrical capacitance was converted to its equivalent fluid capacitance by the following equation:

$$C_f = \frac{C_e}{F c^*} \tag{5}$$

where C_f is the fluid capacitance, C_e the electrical capacitance, F the Faraday, and c^* the concentration change required for a 1-mV change in transepithelial PD. c^* was calculated from the liquid junction potential of two NaCl solutions separated by a barrier. The fluid volume thus determined is a function of the transference numbers of the barrier and for the two cases using the transference numbers for the tight junction [22] is: control 0.4×10^{-5} cm^3 and volume expanded 0.55×10^{-5} cm^3. The anatomic volume of the inter-

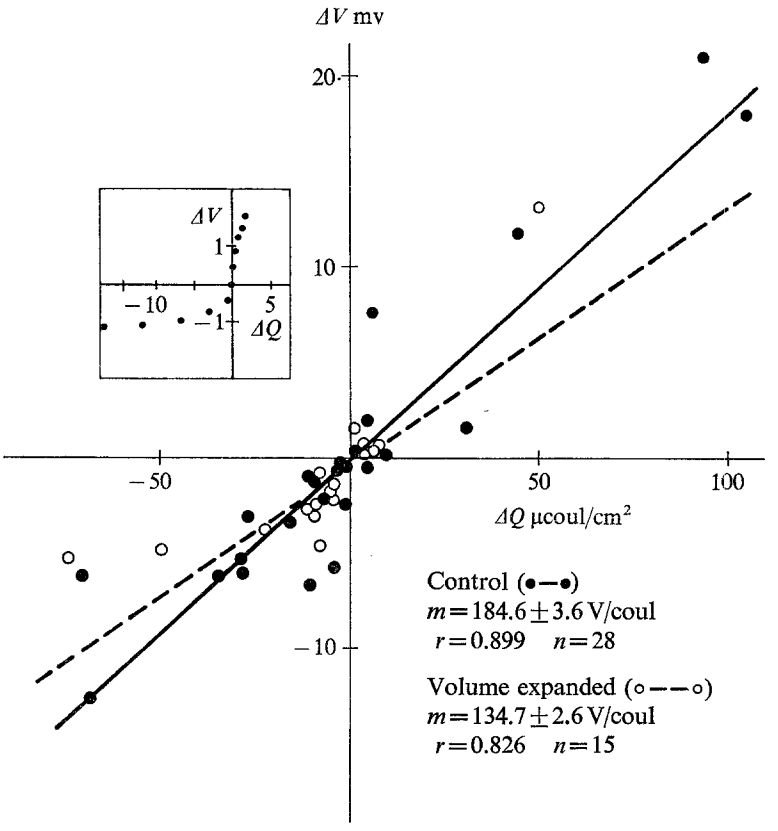

Fig. 8. A graph of the final voltage change (ΔV) induced by current passage versus the integral of the capacitative current (ΔQ) on the abscissa. The filled circles (•) represent control experiments during voltage or current clamp, the open circles (o) represent current clamps carried out while the animal was volume expanded. The lines were drawn by the method of least-squares. Shown in the inset are the results of two individual experiments involving depolarizing command (top) and hyperpolarizing (bottom). The deviation from linearity of the line during hyperpolarization is due to a gradual increase of capacitance as a consequence of current passage

space is about twice as large as this estimate [22, 25] suggesting that only a portion of this space is involved in determining its electrical properties; however, no other known epithelial compartment is of the appropriate volume. The increase in estimated interspace volume during saline loading represents only a modest widening of the intercellular spaces (e. g., from 0.2 to 0.3 μm) and a more dramatic change in capacitance would be expected during higher infusion rates which are known to lead to gross distension of these channels [4].

Also shown in Fig. 8 (inset) are the results of an individual experiment plotted to demonstrate current-induced changes in capacitance. During a depolarizing transient, C did not change significantly, but a hyperpolarizing command caused a deviation from linearity in the graph of ΔV *vs.* ΔQ. The nonlinear hyperpolarizing curve was caused by a gradual increase in capacitance since resistance changes are corrected for by the method described above.

The volume flows which accompany the passage of electric current are always in the direction of cation movement. This observation indicates that the accumulation or depletion of salt within the shunt which leads to the volume flows is critically determined by a barrier whose cation transference number exceeds the free solution value. This point is further discussed in the succeeding paper.

If the shunt pathway in the *Necturus* proximal tubule were simply an unstirred layer of solution, the time constant of the voltage transients during relaxation could be used to calculate the effective diffusion coefficient of NaCl in it. The applicable formula from Crank [9] and Dainty and House [10] is:

$$D_{\text{eff}} = \frac{0.38\,\Delta X^2}{t_{\frac{1}{2}}} \tag{6}$$

where D_{eff} is the effective diffusion coefficient, ΔX is the total thickness of the unstirred layer (in our case equal to about 60 μ) and $t_{\frac{1}{2}}$ the half time of the observed voltage transient (27 sec). D_{eff} equals 0.51×10^{-6} cm^2/sec, nearly 30 times below the free solution value of 1.46×10^{-5} cm^2/sec (20 °C, [19]). This calculation implies that NaCl diffusion in shunt path is markedly restricted, but it is unrealistic to use it to estimate the diffusion coefficient in the shunt. The principle objection to such an attempt is that the lateral space is bounded by "barriers"—e. g., the tight junction and basement membrane—and the shunt cannot be simply represented as an unstirred layer of solution. A more plausible approach is to develop a model of the shunt path which gives a total solute conductance similar to that observed experimentally and which alters with experimental manipulation. The shunt path may be represented by three aqueous barriers to solute movement in a series arrangement: the tight junction, the lateral space itself, and the basement membrane with its associated connective tissue. The total solute conductance of such a series is given by [16]:

$$\frac{1}{\omega_{\text{tot}}} = \frac{1}{\omega_{tj}\gamma_{tj}} + \frac{1}{\omega_{lis}\gamma_{lis}} + \frac{1}{\omega_{bm}\gamma_{bm}} \tag{7}$$

where ω_{tj}, ω_{lis} and ω_{bm} are the NaCl conductance of the tight junction, lateral space, and basement membrane, respectively, and γ_{tj}, γ_{lis}, γ_{bm} are their respective areas per cm^2 of epithelium. For each barrier, representing it as a coarse membrane [15]

$$\omega = \frac{\varphi_w \theta D\,\mathrm{NaCl}}{\Delta X\, 2RT} \tag{8}$$

where φ_w is the water fraction of the barrier which may vary between 0 and 1, θ the tortuosity factor $\leqq 1$, ΔX the barrier thickness, R the gas constant, and T the absolute temperature. I obtain the following values for each permeability:[2]

$$\omega_{tj} = 0.239 \times 10^{-11} \text{ mole/dyne sec}$$

$$\omega_{lis} = 0.99 \times 10^{-14} \text{ mole/dyne sec}$$

$$\omega_{bm} = 0.74 \times 10^{-12} \text{ mole/dyne sec}$$

and $\omega_{\mathrm{tot}} = 0.128 \times 10^{-15}$ mole/dyne sec, or in more commonly used units, 3.1×10^{-6} cm/sec. The total solute conductance is then in agreement with the experimental values [8, 22, 23] when I assume that the NaCl diffusion coefficient is restricted to one-fifth its free solution value. It is apparent that given similar NaCl diffusion coefficients in the tight junction and lateral space, the principal determinant of the shunt path permeability is the lateral space itself since it offers more solute resistance than the other barriers.

These calculations and those that follow in the theoretical treatment of these experiments suggest that changes in the lateral space dimensions significantly affect lateral space volume, shunt solute conductance and shunt electrical conductance. Widening of the lateral space would increase electrical conductance, since, as previously noted by Boulpaep [8] much of the transepithelial electrical resistance may be localized at the level of the lateral

---

2 A summary of the assumptions for each barrier are: 1) tight junction: total linear length of the tight junction per cm^2 of epithelium is 800 cm/cm^2 [8], slit width 25 to 36 Å [4, 5], $\Delta X = 1000$ Å, [4]; assume $\varphi_w = 0.8$, $\theta = 0.5$, and DNaCl $= 0.3 \times 10^{-5}$ cm^2/sec (1/5 of free solution); γ_{tj} is 2.7×10^{-4} cm^2 per cm^2 epithelium. 2) Lateral spaces: width 0.2 μ [5], $\Delta X = 25$ μ [4], $\theta = 0.416$ [25]; assume $\varphi_w = 1$ (fluid filled space), and DNaCl $= 0.3 \times 10^{-5}$ cm^2/sec; γ_{lis} is 1.63×10^{-2} cm^2 per cm^2 epithelium using the same linear length as above (800 cm/cm^2). 3) Basement membrane and adjacent connective tissue: ΔX estimated from the $t_{\frac{1}{2}}$ of voltage transients in peritubular PD observed when capillaries are perfused with high K solution ($t_{\frac{1}{2}} = 5$ sec) as 10 μ for DKCl $= 1.69 \times 10^{-5}$ cm^2/sec [1]; assume $\varphi_w = 1$, $\theta = 1$, DNaCl $= 1.46 \times 10^{-5}$ cm^2/sec (free solution value); and γ_{bm} is 1.45 cm^2 per cm^2 epithelium, calculated from the outside diameter of the tubule.

intercellular space. The fall in transepithelial resistance may be regarded as an indirect measure of the degree of distension of the lateral spaces. A modest widening of the lateral space without alteration of the properties of the tight junction may increase electrical conductance and capacitance proportionally and have virtually no effect on the voltage transient rate constant. An experimental maneuver such as volume expansion which enlarges the lateral spaces [4] would not necessarily lead to changes in the rate constant of the PD transients. During volume expansion in this study, transepithelial resistance fell to three-fourths of its control value, considerably less than the one-third value reported by Boulpaep [8]. A possible explanation for this difference lies in the degree of volume expansion achieved in this study compared to that of Boulpaep since his saline infusion rates were on the average twice those used here. The fall in resistance during saline loading was also less than that observed during hyperpolarizing commands where resistance fell to nearly one-half its original value. During hyperpolarization the volume of the lateral spaces may increase to a greater extent than the conductance, since the resistance of the tight junction is presumably unaffected, leading to a decreased rate constant during hyperpolarization. A nearly threefold decrease in transepithelial input resistance was reported by Windhager *et al.* [26] upon perfusion of the tubule lumen with hypertonic solution (400 mOsm higher than the peritubular solution). A similar resistance decrease (2.2-fold) occurred in the absence of a transepithelial osmotic pressure difference when both luminal and peritubular solutions were made hypertonic. The explanation offered by these authors, cell shrinkage causing a widening of the tight junctions, should on the basis of the preceeding discussion be broadened to include the effects of changes in the interspace width. Hypertonicity which leads to cell volume decrease would also lead to interspace volume increase with concomitant decrease in both solute and electrical resistance.

The shunt path comprises three equivalent electrical elements: a series resistance, variable resistor, and variable capacitor. All three variables are interrelated and combine to determine the properties of the shunt and the time course of the epithelial voltage transients. It is now apparent that the original equation used to fit the voltage transients [Eq. (2)] is a first approximation of a nonlinear function with three variables. The factors which cause the interspace volume to change are as yet undefined and are discussed in greater detail in the second paper of this pair. The overall picture which emerges is one in which lateral space dimensions as well as the properties of the tight junction combine to determine the degree of extracellular shunting and the characteristics of the proximal tubular epithelium.

The author wishes to thank Dr. G. Giebisch for his advice and critical evaluation of this manuscript. This research was supported by NIH training grant No. PHS AM 05644.

References

1. Asterita, M. F. 1971. Electrophysiological estimate of relative thickness of peritubular interstitial space in *Necturus* kidney. *Abstr. Amer. Soc. Nephrol.* p. 5
2. Barry, P. H., Hope, A. B. 1969*a*. Electroosmosis in membranes: Effects of unstirred layers and transport numbers. I. Theory. *Biophys. J.* **9**:700
3. Barry, P. H., Hope, A. B. 1969*b*. Electroosmosis in membranes: Effects of unstirred layers and transport numbers. II. Experimental. *Biophys. J.* **9**:729
4. Bentzel, C. J. 1971. Proximal tubular structure-function relationship during volume expansion in *Necturus* kidney. *Abstr. Amer. Soc. Nephrol.* p. 9
5. Bentzel, C. J., Parsa, B., Hare, D. K. 1969. Osmotic flow across proximal tubule of *Necturus*: Correlation of physiologic and anatomic studies. *Amer. J. Physiol.* **217**:570
6. Boulpaep, E. L. 1967. Ion permeability of the peritubular and luminal membrane of the renal tubule cell. *In:* Symposium über Transport und Funktion intracellulärer Elektrolyte. F. Krück, editor. p. 98 Urban and Schwarzenberg, Berlin
7. Boulpaep, E. L. 1971. Electrophysiological properties of the proximal tubule: Importance of cellular and intercellular transport pathways. *In:* Electrophysiology of Epithelial Cells. G. Giebisch, editor. p. 91. F. K. Schattauer Verlag, Stuttgart
8. Boulpaep, E. L. 1972. Permeability changes of the proximal tubule of *Necturus* during saline loading. *Amer. J. Physiol.* **222**:517
9. Crank, J. 1957. The Mathematics of Diffusion. Oxford University Press, London
10. Dainty, J., House, C. R. 1966. Unstirred layers in frog skin. *J. Physiol.* **182**:66
11. Frizzell, R. A., Schultz, S. G. 1972. Ionic conductances of extracellular shunt pathway in rabbit ileum. *J. Gen. Physiol.* **59**:318
12. Frömter, E. 1972. Progress in microelectrode techniques for kidney tubules. *Yale J. Biol. Med.* **45**:414
13. Frömter, E., Diamond, J. M. 1972. Route of passive ion permeation in epithelia. *Nature, New Biol.* **235**:9
14. Hildebrand, F. B. 1956. Introduction to Numerical Analysis. p. 75. McGraw-Hill Book Co., Inc., New York
15. Kedem, O., Katchalsky, A. 1961. A physical interpretation of the phenomenological coefficients of membrane permeability. *J. Gen. Physiol.* **45**:143
16. Kedem, O., Katchalsky, A. 1963. Permeability of composite membranes. Part 3. Series array of elements. *Trans. Faraday Soc.* **59**:1941
17. Nakajima, K., Clapp, J. R., Robinson, R. R. 1970. Limitations of the shrinking-drop micropuncture technique. *Amer. J. Physiol.* **210**:345
18. Noyes, D. H., Rehm, W. S. 1971. Unstirred-layer model for the long-time-constant transient voltage response to current in epithelial tissue. *J. Theoret. Biol.* **32**:25
19. Robinson, R. A., Stokes, R. H. 1959. Electrolyte Solutions. Butterworths, London
20. Rose, R. C., Schultz, S. G. 1971. Studies on the electrical potential profile across rabbit ileum. *J. Gen. Physiol.* **57**:639
21. Spring, K. R. 1972. Insertion of an axial electrode into renal proximal tubule. *Yale J. Biol. Med.* **45**:426
22. Spring, K. R. 1973. A parallel path model for *Necturus* proximal tubule. *J. Membrane Biol.* **13**:323
23. Spring, K. R., Paganelli, C. V. 1972. Sodium flux in *Necturus* proximal tubule under voltage clamp. *J. Gen. Physiol.* **60**:181

24. Wedner, H. J., Diamond, J. M. 1969. Contributions of unstirred-layer effects to apparent electrokinetic phenomena in the gall-bladder. *J. Membrane Biol.* **1**:92
25. Whittembury, G. 1967. Sobre los mecanismos de absorción en el tubo proximal del riñón. *Acta Cient. Venezolana Suppl.* **3**:71
26. Windhager, E. E., Boulpaep, E. L., Giebisch, G. 1967. Electrophysiological studies on single nephrons. *In:* Proceedings of the International Congress of Nephrology. J. S. Handler, editor. Vol. 1: Physiology. p. 35. S. Karger, Basel